The American Journal of Pathology, Vol. 171, No. 2, August 2007

DOI: 10.2353/ajpath.2007.061251

Vascular Biology, Atherosclerosis and Endothelium Biology

Molecular Changes in the Vasculature of Injured Tissues

Tero A.H. Järvinen* and Erkki Ruoslahti*†

From the Cancer Research Center, Burnham Institute for Medical Research, La Jolla; and Burnham Institute for Medical Research,† University of California, Santa Barbara, California*

We have explored molecular specialization of the vasculature of regenerating wound tissue in the skin and tendons to identify a different repertoire of markers from that obtained by studying tumor vasculature. We screened a phage-displayed peptide library for peptides that home to wounds in mice and identified two peptides that selectively target phage to skin and tendon wounds: CARSKNKDC (CAR) and CRKDKC (CRK). CAR is homologous to heparin-binding sites in various proteins and binds to cell surface heparan sulfate and heparin. CRK is similar to a segment in thrombospondin type 1 repeat. Intravenously injected CAR and CRK phage, as well as fluorescein-labeled CAR and CRK peptides, selectively accumulated at wound sites, where they partially co-localized with blood vessels. The CAR peptide showed a preference for early stages of wound healing, whereas the CRK favored wounds at later stages of healing. The CAR peptide was internalized into the target cells and delivered the fluorescent label into the cell nuclei. These results identify new molecular markers in wound tissues and show that the expression of these markers in wound vasculature changes as healing progresses. The peptides recognizing these markers may be useful in delivering treatments into regenerating tissues. ***(Am J Pathol 2007, 171:702–711; DOI: 10.2353/ajpath.2007.061251)***

Tissue regeneration, inflammation, and tumors induce the growth of new blood vessels from pre-existing ones. This process, angiogenesis, is a vital requirement for wound healing because the formation of new blood vessels allows a variety of mediators, nutrients, and oxygen to reach the healing tissue.[1–3] Newly formed blood vessels differ in structure from pre-existing vasculature. Such differences have been extensively characterized by comparing tumor vasculature to normal vessels.[4–6] Angiogenic vessels in nonmalignant tissues and in premalignant lesions share markers with tumor vessels,[7,8] but distinct markers also exist.[9,10]

Here, we use *in vivo* screening of phage-displayed peptide libraries to probe vascular specialization. This method has revealed a surprising degree of heterogeneity in the vasculature; tissue-specific homing peptides have been identified for a large number of normal organs and tissues,[11–13] and tumors and atherosclerotic lesions have been shown to carry their own vascular markers, both in the blood vessels and in lymphatics.[6,14,15] We reasoned that surveying nonmalignant angiogenesis might reveal a different repertoire of markers than has been obtained by studying tumor vasculature. We chose wounds as the target because wounds are one of the few nontumor locations where angiogenesis takes place in an adult organism.

In this study, we report on two peptides that specifically deliver the phage or peptide-coupled fluorophor to wound microvasculature after intravenous injection. These peptides seem to be different from previously described tumor-homing peptides and they reveal changes in the molecular profile of wound vasculature as the wound heals.

Materials and Methods

Materials

Heparinase I (*Flavobacterium heparinum*; heparin lyase, EC 4.2.2.7), heparinase III (*F. heparinum*; heparin-sulfate lyase,

Supported by the National Cancer Institute (grant CA 82713, CA 119335, and Cancer Center support grant CA 30199); the Department of Defense (grant DAMD17-02-1-03150); the Sigrid Juselius Foundation, Helsinki, Finland (postdoctoral fellowship grants to T.A.H.J.); and the AO Foundation, Switzerland (to T.A.H.J.).

Accepted for publication May 8, 2007.

Supplemental material for this article can be found on *http://ajp.amjpathol.org*.

Curent address of T.A.H.J.: Medical School and Department of Orthopaedic Surgery, University of Tampere and Tampere University Hospital, Tampere, Finland.

Address reprint requests to Erkki Ruoslahti, Burnham Institute for Medical Research at UCSB, 1105 Life Sciences Bldg., Department of Molecular, Cellular, and Developmental Biology, University of California, Santa Barbara, Santa Barbara, CA 93106-9610. E-mail: ruoslahti@burnham.org.

EC 4.2.2.8), and heparin immobilized on acrylic beads were purchased from Sigma-Aldrich (St. Louis, MO).

Generation of Wounds

Wound experiments were performed in 6- to 8-week-old male Sprague-Dawley rats and BALB/c mice. Rats were anesthetized with an intraperitoneal injection of 50/50% ketamine-xylaxine, and an intraperitoneal injection of 2.5% avertin (Sigma-Aldrich) was used for mice. Skin was shaved, cleaned, and disinfected with povidone-iodine (Betadine; Sigma-Aldrich) and 70% alcohol. All animal experiments were approved by the Institutional Animal Care and Use Committee of Burnham Institute for Medical Research.

Two types of injuries were used with patellar tendons. For phage screening in rats, patellar tendons were exposed through small skin incisions placed on the lateral side of the joint, so that the skin wound and tendon wound were not in direct contact with each other. Six longitudinal, full-length incisions were made into the tendon. Full-thickness incision wounds, 1.5 cm in length, were made in skin on the back of the animal. The skin wounds were left uncovered without a dressing. For quantification of phage homing and peptide injections, two size 11 surgical scalpels were placed side-by-side and the central third of the patellar tendon was removed analogous to the graft used in anterior cruciate ligament reconstruction. Achilles tendons were wounded by making four longitudinal, full-length incisions into the tendon. Skin wounds were 8-mm circular, full-thickness excision wounds, made to the skin with a biopsy punch. None of the procedures prevented the animals from bearing weight and moving immediately after the operation and without a noticeable limp.

Phage Libraries, Library Screening, and Individual Phage Clones

The libraries were prepared by using NNK-oligonucleotides encoding a random library of cyclic peptides of the general structure CX_7C (C, cysteine; X, any amino acid). The oligonucleotide mixture was cloned into the T7Select 415-1 vector according to the manufacturer's instructions (Novagen, Madison, WI). This vector displays peptides in all 415 copies of the phage capsid protein as a C-terminal fusion. Libraries with this structure have yielded numerous high-affinity cell-binding peptides.[6,11,16,17]

The screening process involved three *in vivo* selection rounds, performed essentially as described.[17] Eight-week-old Sprague-Dawley rats were injected with the library [1 to 5×10^{11} phage in 1.5 ml of phosphate-buffered saline (PBS)] through the tail vein or intracardially and were perfused 12 minutes later through the heart with 1% bovine serum albumin in Dulbecco's modified Eagle's medium to remove unbound intravascular phage. The short circulation time focused the screening on the blood vessels because the intact phage cannot readily access extravascular tissue. It also minimized any neutralization or processing of the phage in the tissues. The first *in vivo* round included 19 animals with both patellar tendon and skin wounds, which were separately pooled. The second round used separate sets of three animals for tendon and skin wound screening, and the third round was performed with one wound of each kind.

The following primers, expressing the indicated peptides, were used to prepare phage: CAR, 5′-AATTCCTGCGCGCGTTCGAAGAATAAGGATTGCTA-3′ and 5′-AGCTTAGCAATCCTTATTCTTCGAACGCGCGCAGG-3′; CRK, 5′-AATTCCTGCCGGAAGGATAAGTGCTA-3′ and 5′-AGCTTAGCACTTATCCTTCCGGCAGG-3′; CAQSNNKDC, 5′-AATTCCTGCGCGCAGTCGAACAATAAGGATTGCTA-3′ and 5′-AGCTTAGCAATCCTTATTGTTCGACTGCGCGCAGG-3′; CAR2, 5′-AATTCCTGCGCTAGGTCTACTGCTAAGACTTGCTA-3′ and 5′-AGCTTAGCAAGTCTTAGCAGTAGACCTAGCGCAGG-3′; and CRASKC, 5′-AATTCCTGCCGGGCATCTAAGTGCTA-3′ and 5′-AGCTTAGCACTTAGATGCCCGGCAGG-3′. To test single phage clones *in vivo*, 1×10^{10} phage in 1.5 ml of PBS were injected through the tail vein. After the circulation period and perfusion, tissue samples were harvested and weighed. Phage titers per mg of wet tissue were then determined, and the results were expressed as the ratio between the titer of the test clone and nonrecombinant control phage in the same tissue.

Peptides

Peptides were synthesized with an automated peptide synthesizer by using standard solid-phase fluorenylmethoxycarbonyl chemistry. During synthesis, the peptides were labeled with fluorescein using an amino-hexanoic acid spacer as described.[18] Each individual fluorescein-conjugated peptide was injected intravenously into the tail vein of rats or mice with wounds. The peptides were allowed to circulate for different periods of time, followed by heart perfusion. Tissues were embedded into OCT (Tissue-Tek; Sakura Finetek U.S.A., Inc., Torrance, CA) and processed for microscopy.

Immunohistochemistry

Frozen tissue sections were fixed in acetone for 10 minutes and incubated with 0.5% blocking reagent for 1 hour (NEN Life Sciences, Boston, MA). Tissue sections were incubated with the primary antibody overnight at 4°C. The following monoclonal antibodies (mAbs) and polyclonal antibodies (pAbs) were used: rabbit anti-T7-phage affinity-purified pAb (1:100),[17] rat anti-mouse CD31 mAb (1:200; BD Pharmingen, San Diego, CA) and rabbit anti-fluorescein isothiocyanate (FITC) pAb (1:200; Invitrogen, Carlsbad, CA). The primary antibodies were detected with labeled secondary antibodies, and each staining experiment included sections stained with species-matched immunoglobulins as negative controls. The sections were washed several times with PBS, mounted in Vectashield mounting medium with 4,6-diamidino-2-phenylindole (DAPI) (Vector Laboratories, Burlingame, CA) and visualized under an inverted fluorescent or light microscope.

Cell Culture

Chinese hamster ovary cells (CHO-K) were obtained from the American Type Culture Collection (Rockville, MD). The pgsA-745 mutant cell line,[19] which is derived from CHO-K, was kindly provided by Dr. J. Esko (University of California at San Diego, La Jolla, CA). Cells were maintained in α-minimal essential medium and Earle's salt supplemented with 10% fetal bovine serum, 100 μg/ml streptomycin sulfate, 100 U of penicillin G/ml, and 292 μg/ml L-glutamine (Invitrogen).

Cell Binding Assays

Cells were detached with 0.5 mmol/L ethylenediaminetetraacetic acid solution (Irvine Scientific, Santa Ana, CA), washed with PBS, and resuspended in 1% bovine serum albumin plus α-minimal essential medium. For the phage binding experiments, $\sim 1 \times 10^{10}$ phages were added to 15 ml of culture media containing $\sim 1 \times 10^6$ cells in a test tube. The samples were rotated for 2 hours at +4°C. The cells were then washed six times and transferred to a new tube. After a final wash, the cells were counted and cell-bound phage titers were determined. Heparinase treatment of the CHO-K cells was performed using 1.5 IU/ml heparinase I and 1.25 IU/ml heparinase III in serum-free culture media for 2 hours.

Peptide binding to cells was studied essentially as described above for phage. Peptides were tested at 5 μmol/L concentration, with or without 5×10^9 phage. After incubation on ice for 30 minutes, the cells were washed and resuspended with PBS containing 2 μg/ml of propidium iodide (Invitrogen) and analyzed using a FACScan flow cytometer (BD Biosciences, San Jose, CA).

To study peptide internalization, CHO-K cells or human umbilical vein endothelial cells seeded on plastic coverslips were incubated with 10 μmol/L fluorescein-conjugated peptides for 30 minutes to 72 hours, washed three times with PBS, and fixed with 4% paraformaldehyde for 20 minutes at room temperature. After several washes with PBS, the nuclei were visualized by staining with DAPI, and the slides were mounted with ProLong Gold anti-fade reagent (Invitrogen). The images were acquired using Olympus IX81 inverted and Olympus Fluoview FV1000 confocal microscopes (Olympus, Melville, NY). *Z*-stack images were taken by confocal microscope every 1 μm through the cells.

Heparin Binding

To measure phage binding to heparin, heparin-coated acrylic beads 10% (v/v) were suspended in 20 mmol/L Na_2HPO_4 buffer, pH 7.2, containing 0.2 mol/L NaCl.[20] Approximately 5.0×10^9 phage particles were incubated with the beads for 1 hour at room temperature. The beads were washed, transferred to new tube, and bound phage was eluted with 1.2 mol/L NaCl (pH 7.2) and titrated.[20]

Statistical Analysis

Differences between the various treatments were statistically tested using the Student's unpaired *t*-test, whereas the phage homing to wounds versus sham-operated tissues was analyzed using the Student's paired *t*-test. For comparisons of multiple groups, statistical analysis was performed by two-way analysis of variance complemented by the Bonferroni post hoc test for pair-wise comparisons between the test groups. The possible difference in the homing of the different phage clones to wounds was assessed using the log-transformed variables. *P* values of less than 0.05 were considered statistically significant for all tests. The significance level shown refers to two-tailed test.

Results

Identification of Homing Peptides by Phage Display

To identify candidate peptides that home into the vasculature in healing wounds, we screened phage libraries *in vivo*. A T7-phage library (diversity 9×10^8) was intravenously injected into rats 5 days after wounding of the skin and tendons. The 5-day time point was chosen because the number of blood vessels in the healing wound peaks at that time.[21–24] Separate screens for phage that home to tendon or skin wounds yielded phage pools with increased affinity for the target tissues. Sequencing of individual phage clones revealed two candidate homing motifs in the selected pools. The sequence CARSKNKDC (referred to as CAR) and a related sequence CARSTKATC (CAR2) were obtained in a tendon wound screen. BLAST analysis[25] showed that the CAR sequence is similar to the main heparin-binding site (RARKKNKNC) of bone morphogenetic protein 4 (BMP4). Another peptide, CRKDKC, was identified once in each of two independent screens on skin wounds. The CRK sequence shows some similarity with sequences in thrombospondin type 1 and type 3 repeats, which are present in a large number of extracellular matrix proteins. The CRK sequence is shorter than the structure of the CX_7C library would predict; a modified peptide structure is a relatively common occurrence in phage screening.[9] The sequence contains a cysteine residue at both ends, which are likely to form a cyclizing disulfide bond. These clones were chosen for further analysis.

The CAR phage homed 100- to 140-fold more efficiently to wounds in the patellar and Achilles tendons and in the skin than nonrecombinant phage (Figure 1A, solid bars). In contrast, similar numbers of both the CAR phage and control phage were seen in liver, kidney, heart, lung, spleen, normal skin, and normal Achilles and patellar tendons (Figure 1A). Immunohistochemistry showed that the CAR phage primarily co-localized with blood vessels (Supplemental Figure 1, see *http://ajp.amjpathol.org*). CAR2 was less effective as a wound homing phage than CAR (see below).

To confirm the specificity of the homing for wound tissue, we induced wounds in the patellar and Achilles tendons of the left hind limb, while subjecting the tendon areas in the right hind limb to a sham operation. The sham operation consisted of a skin incision that exposed the tendon but left

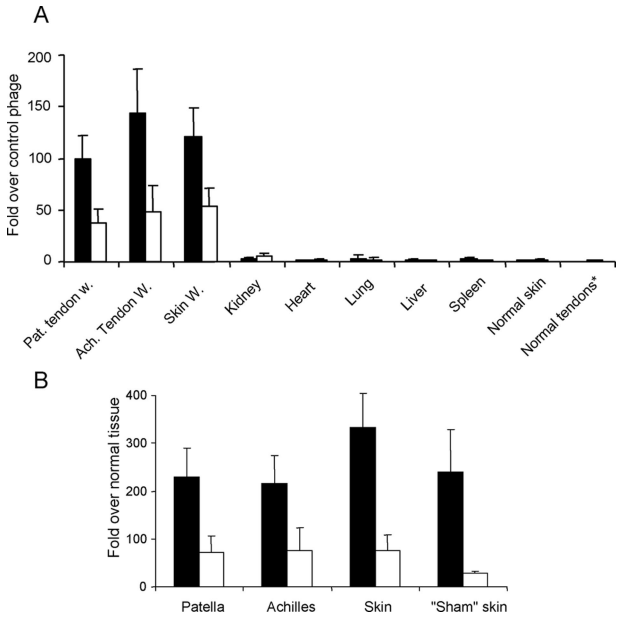

Figure 1. Homing specificity of two wound-homing phage clones. CAR phage (solid bars) or CRK phage (open bars) were injected into rats via tail vein, tissues were dissected 12 minutes later, and phage was recovered and quantified from wounds in patellar and Achilles tendons and skin. Sham-operated (exposed) tendon, normal skin, and other normal tissues were used as controls as indicated. Results are expressed as fold titers relative to that of similarly injected nonrecombinant T7 phage (**A**) or sham-operated contralateral tendon or normal skin after adjusting the output for the wet weight of the tissue samples (**B**). Sham skin refers to skin incision wounds made on the lateral side of the right knee, when the patellar tendon was exposed in the sham-operation. Error bars represent mean ± SEM of 11 experiments for wounds and 4 experiments for control tissues. **A:** Two-way analysis of variance; **B:** paired Student's *t*-test. Both the CAR and CRK phage homed to each of the wound tissues significantly more strongly ($P < 0.001$ or smaller) than the control (nonrecombinant) phage. The CAR phage showed significantly stronger homing than CRK phage to all wounds ($P < 0.01$ or smaller). Normal tendons* indicates combined data from normal Achilles and patellar tendons.

it otherwise intact. We compared *in vivo* phage homing to wounded tissue versus the corresponding normal tissue in the same animal in this model. On day 5 after wounding, the CAR phage homed 220- to 370-fold more to the wounded tendons compared with the contralateral intact tendons and to wounded skin compared with intact skin distant from the wound sites (Figure 1B, solid bars).

Intravenously injected CRK phage homed to 5-day tendon and skin wounds ~50 times more than nonrecombinant control phage (Figure 1A, open bars; and Supplemental Figure 2, see *http://ajp.amjpathol.org*). Comparison to the corresponding healthy tissues on the contralateral side showed nearly 80-fold preference for tendon and skin wounds (Figure 1B, open bars). In contrast, there were no significant differences between CRK phage and control phage in samples recovered from the liver, kidney, heart, lung, spleen, normal skin, or normal tendons (Figure 1A). Like the CAR phage, the CRK phage co-localized with blood vessels (Supplemental Figure 2, see *http://ajp.amjpathol.org*). Finally, we also recloned both the CAR and CRK sequences into the T7 vector and showed that the resulting phage clones homed to wounds as effectively as the original phage (the homing data obtained with the original and new phage clones have been pooled in Figure 1).

Sequence Specificity of Wound Homing by CAR and CRK

In the same tendon wound screen that produced the CAR sequence, we identified a peptide with a somewhat related sequence, CARSTKATC (CAR2). We generated a CAR mutant phage by changing two basic amino acids to neutral ones (CA*R*S*K*NKDC mutated to CA*Q*S*N*NKDC). Both CAR2 and the mutant phage showed impaired wound-homing properties: the CAR2 phage had ~20% of the homing activity of CAR and the mutant phage was essentially inactive in homing (Supplemental Figure 3, A–C, see *http://ajp.amjpathol.org*). We also generated a mutant CRK phage by changing two amino acids (from CR*KD*KC to CR*AS*KC). The mutant phage had also almost completely lost the homing ability (Supplemental Figure 3, A–C, see *http://ajp.amjpathol.org*). The loss of activity as a result of the sequence changes emphasizes the role of the basic amino acids in the homing activity and attests to the specificity of the homing.

Synthetic CAR and CRK Peptides Accumulate in Wounds

We synthesized the CAR and CRK peptides as fluorescein (FITC) conjugates and tested their tissue distribution after intravenous injection to mice and rats with tendon and skin wounds. Both peptides produced strong fluorescent signal in the wounds that partially co-localized with CD31-positive cells at 4 and 8 hours after the injection (Figures 2 and 3). CAR2, even though slightly active at the phage-homing level, produced no accumulated fluorescence, and an unrelated five amino acid control peptide (KAREC) also gave no detectable signal in the wounds. Because of an autofluorescent background in wounds, the fluorescein-labeled peptides were also detected with an anti-FITC antibody, and the signal was thus amplified and converted to a nonfluorescent dye. The antibody staining confirmed the localization of the fluorescein label in the granulation tissue, particularly at later time points when the fluorescent signal was weak. The fluorescent signal produced by CAR and CRK in nontumor tissues (liver, kidney, lung, and spleen) did not differ from that of the fluorescein-labeled CAR2 or KAREC peptides used as controls (Supplemental Figure 4A, see *http://ajp.amjpathol.org*). In agreement with the phage results, no CAR or CRK peptide accumulated in normal skin (Supplemental Figure 4B, see *http://ajp.amjpathol.org*) or tendons (not shown).

Healing Stage-Dependent Changes in Phage Homing

To determine the extent our wound-homing peptides would home to wounds at times other than the 5-day time point, we injected individual phage clones at days 7, 10, and 14, after wounding. The total number of homing phage rescued from the wounds decreased by two orders of magnitude as wound healing progressed

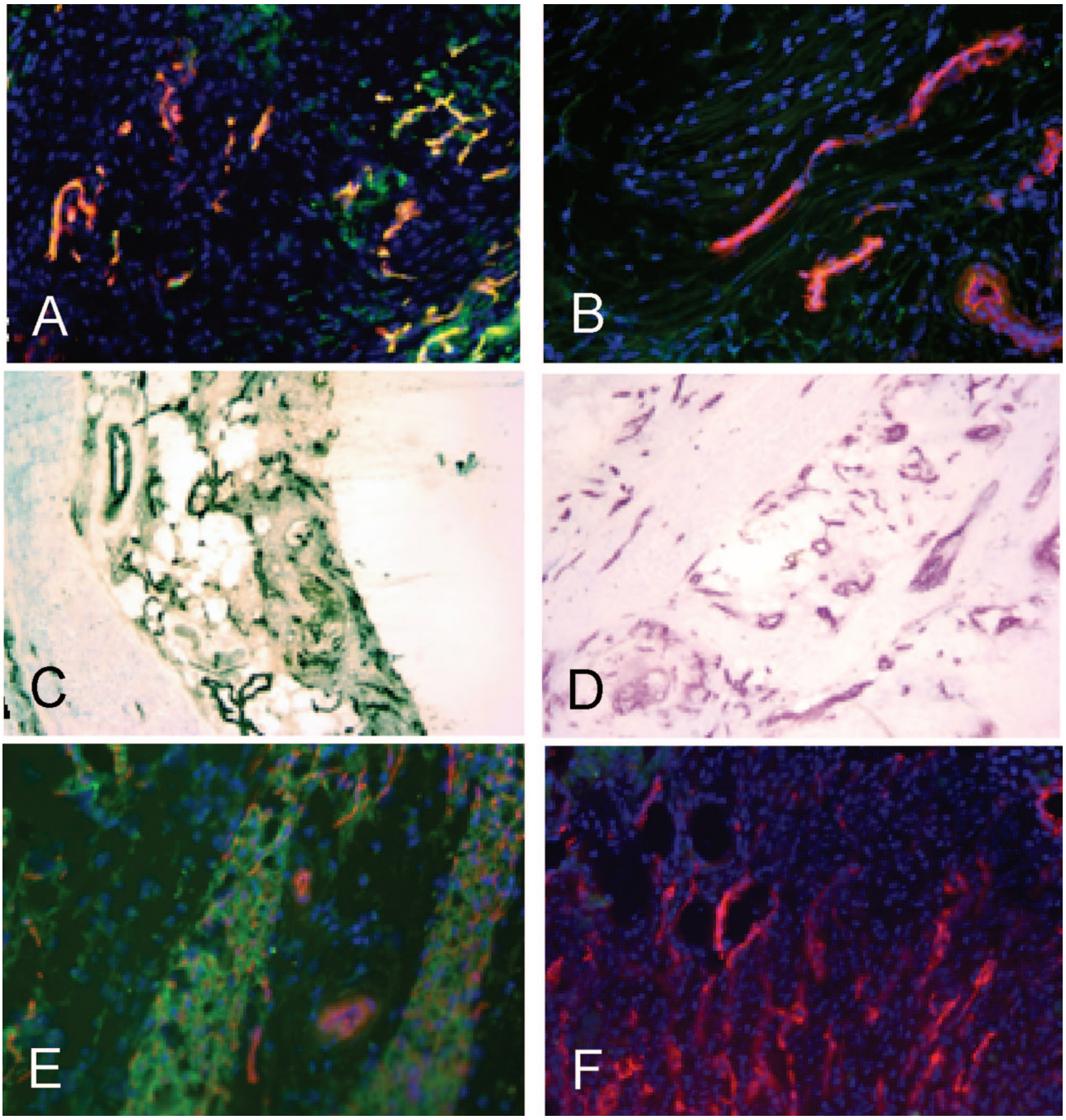

Figure 2. CAR peptide homes to blood vessels and granulation tissue in tendon and skin wounds. Fluorescein-conjugated peptides CAR (**A**, **C**, and **E**) or CAR2 (**B**, **D**, and **F**) were intravenously injected into rats (**A–D**) or mice (**E** and **F**) with 5-day-old wounds in Achilles tendons (**A–D**) or skin (**E** and **F**). Wound tissue was collected 4 hours later, which allowed the peptide to penetrate into the tissue, and examined for the presence of the peptides. In **A–D**, rabbit anti-FITC followed by FITC-conjugated (**A** and **B**) or biotin-conjugated anti-rabbit IgG and streptavidin peroxidase (**C** and **D**; brown), were used to detect the signal from the fluorescein-labeled peptide. Blood vessels were stained with CD-31 antibody (magenta in **C** and **D**) and the nuclei were stained with DAPI (blue). Original magnifications, ×200.

(not shown), presumably reflecting the pruning that occurs in wound vasculature during the maturation of granulation tissue into scar tissue.[3] However, comparison with control phage revealed selective homing even at the late (day 14) stages of wound healing (Figure 4). The CRK phage, which homed less strongly than CAR on day 5, was generally the more efficient homing peptide at the later stages of wound healing. Phage staining showed that both phage clones co-localized with blood vessels at all stages in wound healing (Supplemental Figures 1 and 2, see *http://ajp.amjpathol.org*), and in agreement with the phage homing data, little CAR phage was detected in 14-day wounds, whereas the CRK phage still gave relatively strong staining at this stage (Supplemental Figure 5, see *http://ajp.amjpathol.org*). The co-localization of the phage staining indicates that the molecular change reflected in the relative homing of CAR and CRK re-

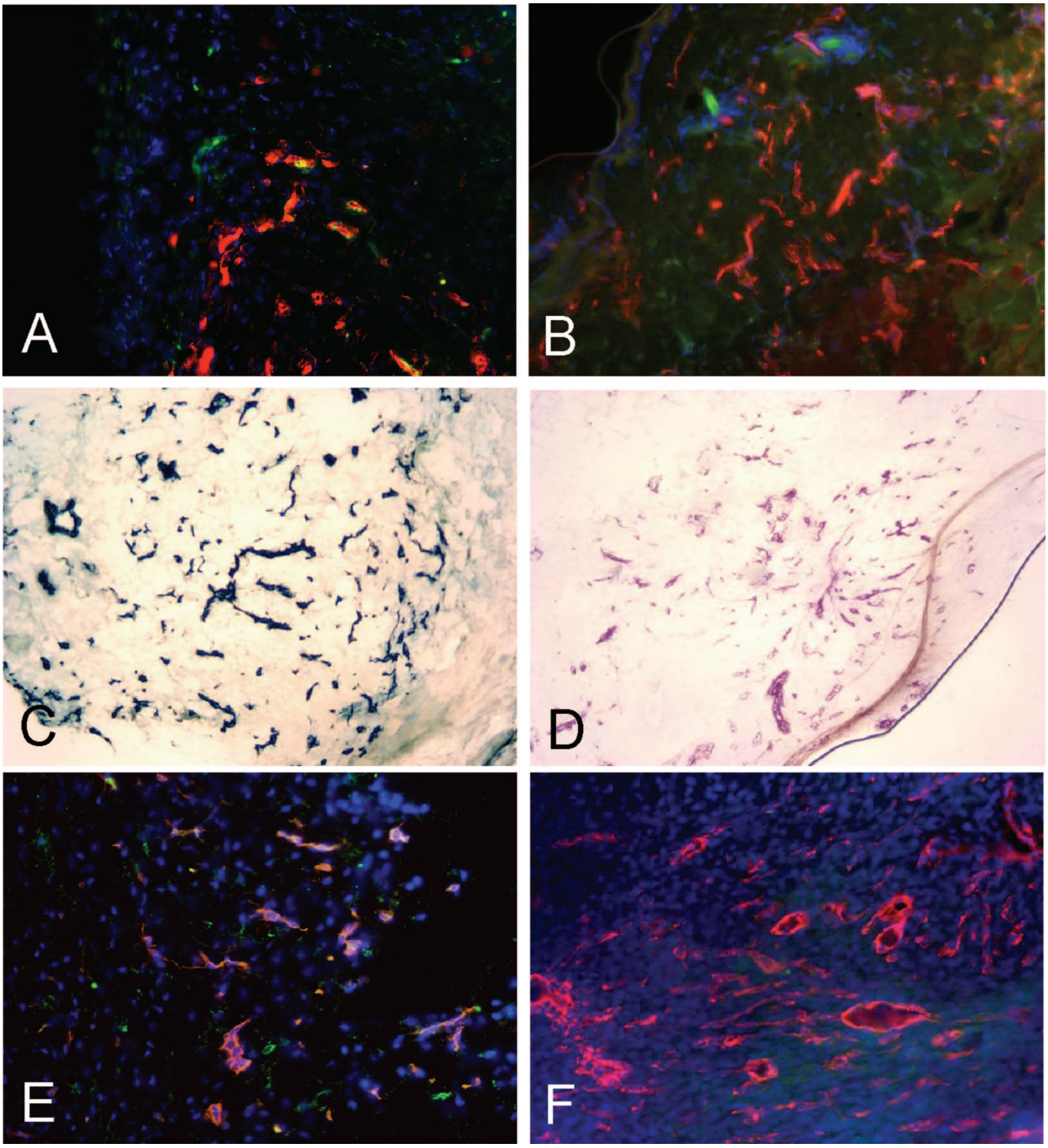

Figure 3. CRK peptide homes to blood vessels and granulation tissue in wounds. Fluorescein-conjugated peptides CRK (**A**, **C**, and **E**) or KAREC (control peptide: **B**, **D**, and **F**), were intravenously injected as in Figure 2 into rats (**A** and **B**) or mice (**C–F**) with 5-day-old wounds in the skin (**A–D**) or patellar tendons (**E** and **F**). The peptides, blood vessels, and nuclei were detected as in Figure 2. Original magnifications, ×200.

sides in the vasculature and that this change is related to the maturation of the vasculature in wounds.

Cell Surface Heparan Sulfate as the Target Molecule for CAR

The CAR sequence homology with the heparin-binding site of BMP4 and the presence in CRK of a classical heparin-binding motif (XBBXBX; where X denotes any amino acid and B basic residue), suggested that a particular form of a glycosaminoglycan, probably a heparan sulfate, might serve as the binding site for one or both of the peptides. We used Chinese hamster ovary cells (CHO-K) and the pgsA-745 mutant CHO line that is defective in glycosaminoglycan biosynthesis[19] to test the binding of CAR and CRK to cell surface

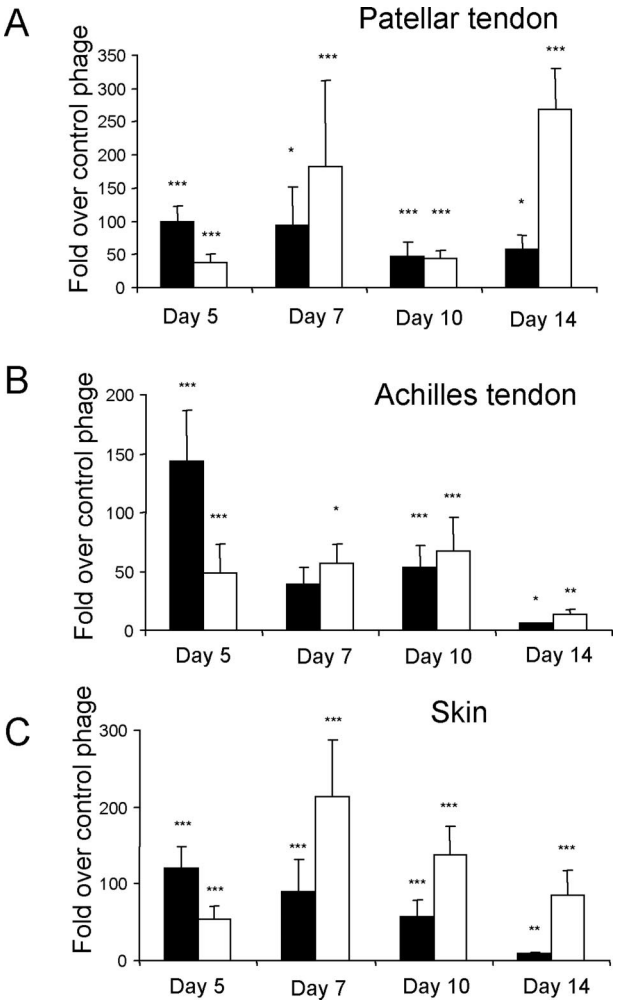

Figure 4. Healing stage dependence of phage homing to wounds. CAR phage (filled bars) or CRK phage (open bars) was intravenously injected into rats 5, 7, 10, and 14 days after wounding. The phage was recovered 12 minutes after the injection and quantified. Results are expressed as fold titers relative to that of similarly injected nonrecombinant T7 phage after adjusting the output to the wet weight of the tissue samples. **A:** Patellar tendon wounds; **B:** Achilles tendon wounds; **C:** skin wounds. The CAR and CRK phage homing shows a different healing time dependence. Error bars represent mean ± SEM for 11, four, seven, and five separate experiments at each time point. $^{*}P < 0.05$, $^{**}P < 0.01$, $^{***}P < 0.001$ versus nonrecombinant T7 phage, two-way analysis of variance.

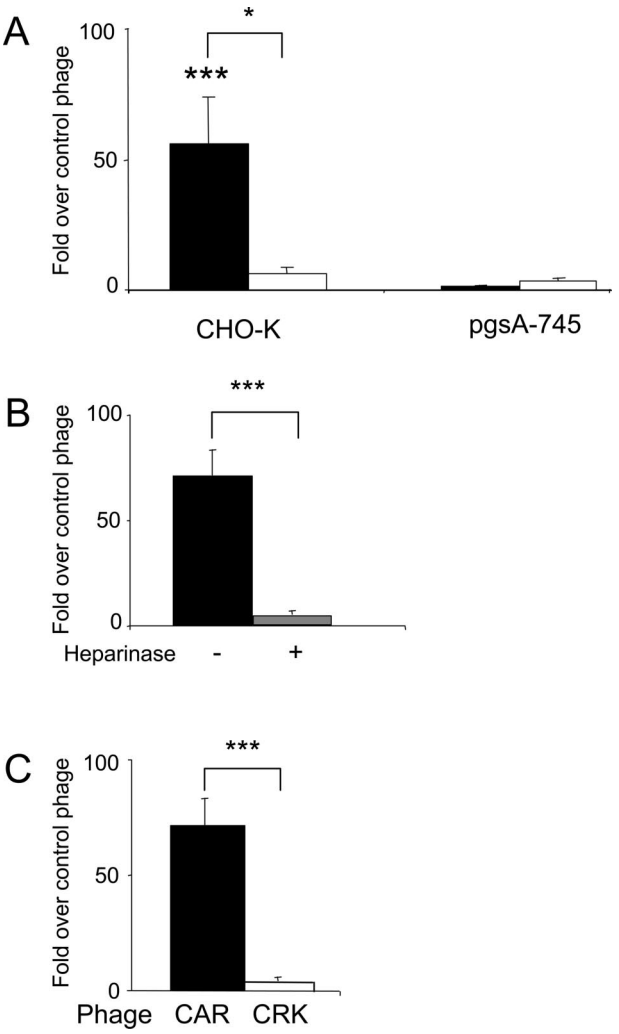

Figure 5. Binding of CAR phage to cell surface heparan sulfate and heparin. **A:** CAR phage (filled bars) specifically binds to CHO-K cells, but not to the glycosaminoglycan-deficient pgsA-745 cells. CRK phage (open bars) does not bind significantly to either cell line. **B:** Heparinase treatment of the CHO-K cells (gray bar) suppresses the binding of the CAR phage to these cells. **C:** CAR phage, but not CRK phage, binds to heparin-coated beads. Error bars represent mean ± SEM for three or more separate experiments performed in duplicate. $^{*}P < 0.05$; $^{***}P < 0.001$. **A** and **B:** Two-way analysis of variance; **C:** unpaired Student's *t*-test. Brackets indicate the difference between CAR and CRK phages.

glycosaminoglycans. CAR phage bound to the CHO-K cells 55-fold more than nonrecombinant control phage ($P < 0.0001$), but there was no specific binding to the glycosaminoglycan-deficient cells (Figure 5A). The CRK phage did not bind significantly to either cell line (Figure 5A). Pretreatment of the CHO-K cells with heparinase I and III decreased the binding of the CAR phage by almost 80% ($P < 0.0001$; Figure 5B). The CAR phage also bound to heparin-coated beads; 70-fold more CAR phage than nonrecombinant control phage was recovered from the beads ($P < 0.0001$; Figure 5C). CRK phage binding was only marginally higher than that of the control phage.

Fluorescence-activated cell sorting analysis also revealed strong binding of the synthetic CAR peptide to the CHO-K cells, but not to the pgsA-745 cells. An excess of unlabeled CAR peptide inhibited the binding in a dose-dependent manner. The binding could also be inhibited with the CAR phage. The CAR2 peptide bound only weakly to the CHO-K cells, and KAREC showed no binding to either the CHO-K or pgsA-745 cells (data not shown). These results indicate that CAR, but not CRK, has an active heparin-binding site, and that CAR binds to glycosaminoglycan moiety in cell surface heparan sulfate proteoglycans.

Cell-Penetrating Properties of CAR Peptide

Many of the best-characterized cell penetrating peptides contain basic residues, and heparan sulfate proteoglycans are thought to be involved in the internalization of these peptides.[26,27] This prompted us to study the cell-penetrating properties of the wound-

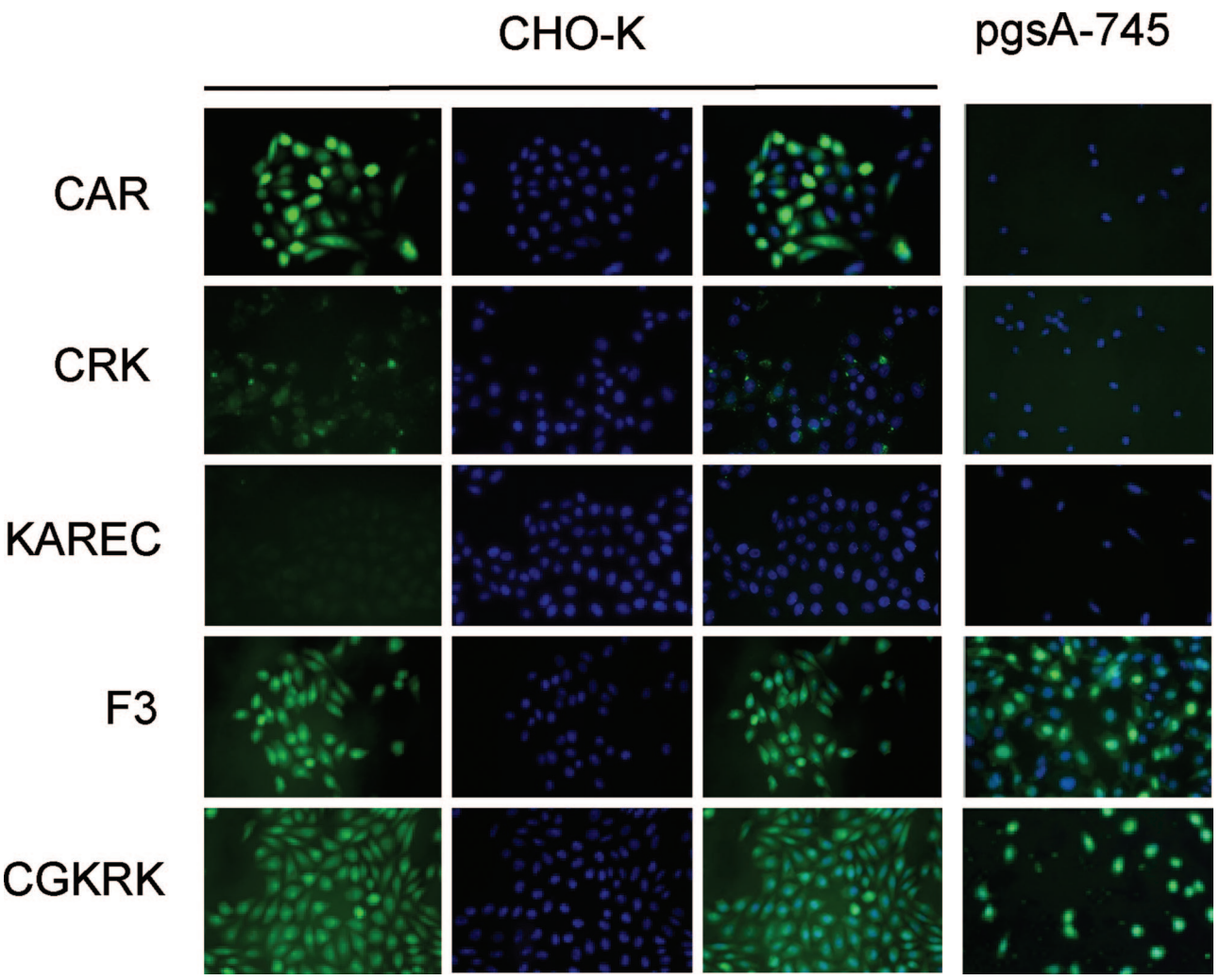

Figure 6. The CAR peptide is internalized into CHO-K cells. Fluorescein-conjugated peptides as indicated were incubated at 10 μmol/L concentration with CHO-K and pgsA-745 cells for 24 hours. The cells were washed, fixed, stained with the nuclear stain DAPI (blue; CHO-K panels, middle), and examined for green fluorescence from the labeled peptides. The CAR peptide produces strong green fluorescence in the CHO-K cells that mostly overlaps with nuclear DAPI staining (right). This peptide does not appear in the glycosaminoglycan-deficient pgsA-745 cells. The CRK peptide binds weakly to the CHO-K cells. No overlap with nuclei is evident. KAREC control peptide gives no detectable cellular fluorescence, whereas F3 and CGKRK internalize in both CHO-K and pgsA-745 cells, overlapping with nuclei. Original magnifications, ×400.

homing peptides. Fluorescence from labeled CAR peptide incubated with CHO-K cells accumulated within 30 minutes inside the cells, overlapping with the nucleus (Figure 6). Confocal microscopy (not shown) confirmed the nuclear localization. The CRK peptide slightly bound to the cells but was not detectably internalized. The KAREC control peptide (Figure 6) or CAR2 (not shown) did not bind or become internalized. That the CAR peptide neither bound nor internalized into the glycosaminoglycan-deficient pgsA-745 cells (Figure 6), confirmed the specificity of the internalization and its dependence on the binding of the CAR peptide to its receptor. Thus, the CAR peptide seems to be a cell-penetrating peptide.

We have previously characterized two cell-penetrating peptides, CGKRK and F3, that specifically recognize angiogenic endothelial cells and tumor cells.[9,28] Each of these peptides contains basic residues, raising the question of whether they might bind to the same sites at the cell surface as the CAR peptide. F3 and CGKRK accumulated in the cytosol and nuclei of both the CHO-K and pgsA-745 cells (Figure 6), whereas CAR only bound to and was internalized by the CHO-K cells (and CRK did not bind avidly to either cell line). Moreover, a 10-molar excess of unlabeled F3 or CGKRK peptide did not detectably affect the uptake fluorescein-label from the CAR peptide by the CHO-K cells (not shown). Taken together with our previous demonstration that the receptor for the F3 peptide is cell surface-expressed nucleolin,[29] rather than heparan sulfate, these results show that the specificities of CAR and CRK are novel.

Discussion

We report here two novel peptides that specifically home to tendon and skin wounds, targeting both the vasculature and granulation tissue of the wounds. The target

molecule of one of the peptides seems to be a cell surface heparan sulfate structure. We use these peptides to provide evidence that the molecular profile of blood vessels in wounds changes as wounds mature.

In this work we used *in vivo* screening of phage libraries, which primarily probes the blood vessels.[6,11] Our approach was based on the notion that using wound-induced angiogenesis as a target might produce a different repertoire of vascular homing peptides than screening on other types of angiogenic lesions, such as tumors, which have been used extensively in similar screenings.[6] The hypothesis may have been correct, at least to the extent that the two peptides we have isolated seem to be unique. Our wound-homing peptides contain several basic residues, and highly basic peptides have been previously identified in tumor screens.[9,10,28,30] Moreover, the CAR and CKR peptides also recognize tumor vasculature (T.J. and E.R., unpublished results). However, the arrangement of the basic amino acids and other sequence features distinguish our new peptides from the previously described ones. They also differ in heparin binding and cell-type specificity. Among the earlier peptides, F3 and CGKRK bind to heparin, but as shown here, are equally effective in binding to cells that express cell surface heparan sulfate and cells that lack it. In contrast, CAR does not recognize the heparan sulfate-deficient cells, and CRK does not bind to heparin.

We performed the phage screening using wounds made in two tissues, tendon and skin. The CAR peptide came from a tendon screen and the CRK peptide was obtained in a skin screen. Despite their different origin, both peptides homed to wounds in both tissues, indicating that if vascular markers specific for individual tissues exist, our screening did not reveal such markers. However, our screening strategy of using the peak of angiogenesis might not have been ideal for revealing tissue-specific differences. Wounds that have healed sufficiently to regain elements of the original tissue may be more likely to reveal tissue-specific angiogenesis markers. In addition, the molecular changes detected by CAR and CRK may not be exclusively expressed in blood vessels; the fluorescein-labeled peptides, and to some extent the phage clones, spread into extravascular wound tissue, suggesting that cells in the granulation tissue may also express the receptors for these peptides.

The CAR and CRK peptides displayed an opposite homing preference with regard to the age of the wound; CAR favors early wounds and CRK prefers mature ones. Although the CAR peptide homing was clearly transient during wound healing, we did not follow the wounds long enough to see CRK homing disappear, but it seems likely that CRK homing is also transient. Because the phage almost exclusively accumulated in the wound blood vessels, we conclude that wound maturation is accompanied by changes in the profile of molecular markers in wound blood vessels. This conclusion parallels what has been observed in studies on tumor vasculature. Vascular markers can distinguish the blood vessels and lymphatics in premalignant lesions from those of fully malignant tumors in the same tumor system.[10,12] Furthermore, blood vessels in tumors at different stages of tumor development and different stages of vessel maturation differ in their response to anti-angiogenic treatments.[31,32] Our results show that a similar maturation process takes place in wound vasculature. Individual vessels in a wound may not all be at the same stage in the maturation process because there were always some vessels in otherwise positive samples that did not bind the peptides.

The CAR peptide binds to heparin and cell surface heparan sulfate, suggesting that one or more heparan sulfate proteoglycans at the cell surface are the target molecules for this peptide. Heparan sulfate proteoglycans are ubiquitously expressed, but sequence variability in their heparan sulfate component makes possible tissue and cell type-specific interaction with proteins.[20,33–35] The specificity of the CAR peptide for wound vessels and tumor vessels suggests that this peptide may recognize a heparan sulfate sequence specific for wound and tumor angiogenesis. The CRK peptide showed some homology with sequences in thrombospondin type 1 and type 3 repeats, but it is unlikely that this peptide would bind to CD36, which is a known thrombospondin receptor in endothelial cells, because the CRK sequence shows no similarity with the thrombospondin sequence that binds CD36 (VTCG[36,37]); the receptor for CRK remains to be identified and is the subject of future studies.

Finally, the peptides we describe here may offer new therapeutic opportunities. Specific targeting of drugs and other therapeutic moieties to injured tissues may be a valuable option, especially when local treatment is not an option. We are exploring this aspect in ongoing work.

Acknowledgments

We thank Drs. Teppo Järvinen, Hannele Uusitalo-Järvinen, and Eva Engvall for comments on the manuscript; Dr. Yoav Altman for help with fluorescence-activated cell sorting analysis; and Robin Newlin, Kang Liu, Buddy and Adriana Charbono, and Kelly McKaig for providing excellent technical assistance.

References

1. Folkman J: Angiogenesis. Annu Rev Med 2006, 57:1–18
2. Falanga V: Wound healing and its impairment in the diabetic foot. Lancet 2005, 366:1736–1743
3. Martin P: Wound healing—aiming for perfect skin regeneration. Science 1997, 276:75–81
4. Wickström S, Keski-Oja J, Alitalo K: Matrix reloaded to circulation hits the tumor target. Cancer Cell 2003, 3:513–514
5. St. Croix B, Rago C, Velculescu V, Traverso G, Romans KE, Montgomery E, Lal A, Riggins GJ, Lengauer C, Vogelstein B, Kinzler KW: Genes expressed in human tumor endothelium. Science 2000, 289:1197–1202
6. Ruoslahti E: Specialization of tumour vasculature. Nat Rev Cancer 2002, 2:83–90
7. Friedlander M, Theesfeld CL, Sugita M, Fruttiger M, Thomas MA, Chang S, Cheresh DA: Involvement of integrins $\alpha v\beta 3$ and $\alpha v\beta 5$ in ocular neovascular diseases. Proc Natl Acad Sci USA 1996, 93:9764–9769
8. Gerlag DM, Borges E, Tak PP, Ellerby HM, Bredesen DE, Pasqualini R, Ruoslahti E, Firestein GS: Suppression of murine collagen-induced arthritis by targeted apoptosis of synovial neovasculature. Arthritis Res 2001, 3:357–361

9. Hoffman JA, Giraudo E, Singh M, Zhang L, Inoue M, Porkka K, Hanahan D, Ruoslahti E: Progressive vascular changes in a transgenic mouse model of squamous cell carcinoma. Cancer Cell 2003, 4:383–391
10. Joyce JA, Laakkonen P, Bernasconi M, Bergers G, Ruoslahti E, Hanahan D: Stage-specific vascular markers revealed by phage display in a mouse model of pancreatic islet tumorigenesis. Cancer Cell 2003, 4:393–403
11. Rajotte D, Arap W, Hagedorn M, Koivunen E, Pasqualini R, Ruoslahti E: Molecular heterogeneity of the vascular endothelium revealed by in vivo phage display. J Clin Invest 1998, 102:430–437
12. Zhang L, Hoffman JA, Ruoslahti E: Molecular profiling of heart endothelial cells. Circulation 2005, 112:1601–1611
13. Kolonin MG, Sun J, Do KA, Vidal CI, Ji Y, Baggerly KA, Pasqualini R, Arap W: Synchronous selection of homing peptides for multiple tissues by in vivo phage display. FASEB J 2006, 20:979–981
14. Liu C, Bhattacharjee G, Boisvert W, Dilley R, Edgington T: In vivo interrogation of the molecular display of atherosclerotic lesion surfaces. Am J Pathol 2003, 163:1859–1871
15. Zhang L, Giraudo E, Hoffman JA, Hanahan D, Ruoslahti E: Lymphatic zip codes in premalignant lesions and tumors. Cancer Res 2006, 66:5696–5706
16. Koivunen E, Wang B, Ruoslahti E: Phage libraries displaying cyclic peptides with different ring sizes: ligand specificities of the RGD-directed integrins. Biotechnology 1995, 13:265–270
17. Laakkonen P, Porkka K, Hoffman JA, Ruoslahti E: A tumor-homing peptide with a lymphatic vessel-related targeting specificity. Nat Med 2002, 8:751–755
18. Laakkonen P, Akerman ME, Biliran H, Yang M, Ferrer F, Karpanen T, Hoffman RM, Ruoslahti E: Antitumor activity of a homing peptide that targets tumor lymphatics and tumor cells. Proc Natl Acad Sci USA 2004, 101:9381–9386
19. Esko JD, Stewart TE, Taylor WH: Animal cell mutants defective in glycosaminoglycan biosynthesis. Proc Natl Acad Sci USA 1985, 82:3197–3201
20. El-Sheikh A, Liu C, Huang H, Edgington TS: A novel vascular endothelial growth factor heparin-binding domain substructure binds to glycosaminoglycans in vivo and localizes to tumor microvascular endothelium. Cancer Res 2002, 62:7118–7123
21. Järvinen M: Healing of a crush injury in rat striated muscle. 3. A microangiographical study of the effect of early mobilization and immobilization on capillary ingrowth. Acta Pathol Microbiol Scand 1976, 84A:85–94
22. Thompson WD, Harvey JA, Kazmi MA, Stout AJ: Fibrinolysis and angiogenesis in wound healing. J Pathol 1991, 165:311–318
23. Dyson M, Young SR, Hart J, Lynch JA, Lang S: Comparison of the effects of moist and dry conditions on the process of angiogenesis during dermal repair. J Invest Dermatol 1992, 99:729–733
24. Paavonen K, Puolakkainen P, Jussila L, Jahkola T, Alitalo K: Vascular endothelial growth factor receptor-3 in lymphangiogenesis in wound healing. Am J Pathol 2000, 156:1499–1504
25. Altschul SF, Madden TL, Schaffer AA, Zhang J, Zhang Z, Miller W, Lipman DJ: Gapped BLAST and PSI-BLAST: a new generation of protein database search programs. Nucleic Acid Res 1997, 25:3389–3402
26. Joliot A: Transduction peptides within naturally occurring proteins. Sci STRE 2005, 313: pe54
27. Zorko M, Langel U: Cell penetrating peptides: mechanism and kinetics of cargo delivery. Adv Drug Deliv Rev 2005, 57:529–545
28. Porkka K, Laakkonen P, Hoffman JA, Bernasconi M, Ruoslahti E: A fragment of the HMGN2 protein homes to the nuclei of tumor cells and tumor endothelial cells in vivo. Proc Natl Acad Sci USA 2002, 99:7444–7449
29. Christian S, Pilch J, Akerman ME, Porkka K, Laakkonen P, Ruoslahti E: Nucleolin expressed at the cell surface is a marker of endothelial cells in angiogenic blood vessels. J Cell Biol 2003, 163:871–878
30. Zurita AJ, Troncoso P, Cardo-Vila M, Logothetis CJ, Pasqualini R, Arap W: Combinatorial screenings in patients: the interleukin-11 receptor as a candidate target in the progression of human prostate cancer. Cancer Res 2004, 64:435–439
31. Casanovas O, Hicklin DJ, Bergers G, Hanahan D: Drug resistance by evasion of antiangiogenic targeting of VEGF signaling in late-stage pancreatic islet tumors. Cancer Cell 2005, 8:299–309
32. Jain RK: Normalization of tumor vasculature: an emerging concept in antiangiogenic therapy. Science 2005, 307:58–62
33. van den Born J, Salmivirta K, Henttinen T, Ostman N, Ishimaru T, Miyaura S, Yoshida K, Salmivirta M: Novel heparan sulfate structures revealed by monoclonal antibodies. J Biol Chem 2005, 280: 20516–20523
34. Freeman C, Liu L, Banwell MG, Brown KJ, Bezos A, Ferro V, Parish CR: Use of sulfated linked cyclitols as heparin sulfate mimetics to probe the heparin/heparin sulfate binding specificity of proteins. J Biol Chem 2005, 280:8842–8849
35. Kreuger J, Spillmann D, Li JP, Lindahl U: Interactions between heparin sulfate and proteins; the concept of specificity. J Cell Biol 2006, 174:323–327
36. Dawson DW, Frieda S, Pearce A, Zhong R, Silverstein RL, Frazier WA, Bouck NP: CD36 mediates the in vitro inhibitory effects of thrombospondin-1 on endothelial cells. J. Cell Biol 1997, 138:707–717
37. Iruela-Arispe ML, Lombardo M, Krutzsch HC, Lawler J, Roberts DD: Inhibition of angiogenesis by thrombospondin-1 is mediated by 2 independent regions within the type 1 repeats. Circulation 1999, 100:1423–1431